

Synthesis, characterization and thermal studies on metal complexes of new azo compounds derived from sulfa drugs

Gehad G. Mohamed^{a,*}, Mohamed A.M. Gad-Elkareem^b

^a Chemistry Department, Faculty of Science, Cairo University, Giza, Egypt

^b Chemistry Department, Faculty of Science, Al-Azhar University, Assiut, Egypt

Received 14 October 2006; accepted 12 January 2007

Abstract

Four new azo ligands, L1 and HL2–4, of sulfa drugs have been prepared and characterized. $[\text{MX}_2(\text{L1})(\text{H}_2\text{O})_m] \cdot n\text{H}_2\text{O}$; $[(\text{MX}_2)_2(\text{HL2 or HL3})(\text{H}_2\text{O})_m] \cdot n\text{H}_2\text{O}$ and $[\text{M}_2\text{X}_3(\text{L4})(\text{H}_2\text{O})] \cdot n\text{H}_2\text{O}$; M = Co(II), Ni(II) and Cu(II) (X = Cl) and Zn(II) (X = AcO); $m = 0-4$ and $n = 0-3$, complexes were prepared. Elemental and thermal analyses (TGA and DTA), IR, solid reflectance spectra, magnetic moment and molar conductance measurements have accomplished characterization of the complexes. The IR data reveal that HL1 and HL2–3 ligands behave as a bidentate neutral ligands while HL4 ligand behaves as a bidentate monoionic ligand. They coordinated to the metal ions via the carbonyl O, enolic sulfonamide $-\text{S}(\text{O})\text{OH}$, pyrazole or thiazole N and azo N groups. The molar conductance data reveal that the chelates are non-electrolytes. From the solid reflectance spectra and magnetic moment data, the complexes were found to have octahedral, tetrahedral and square planar geometrical structures. The thermal behaviour of these chelates shows that the water molecules (hydrated and coordinated) and the anions are removed in a successive two steps followed immediately by decomposition of the ligand in the subsequent steps. The activation thermodynamic parameters, such as, E^* , ΔH^* , ΔS^* and ΔG^* are calculated from the TG curves applying Coats–Redfern method.

© 2007 Published by Elsevier B.V.

Keywords: Sulfa drugs; Metal complexes; IR; Conductance; Solid reflectance; Magnetic moment; Thermal analysis

1. Introduction

Aromatic sulfonamide derivatives exhibit a range of bioactivities, including anti-angiogenic [1,2], anti-tumor [2,3], anti-inflammatory and anti-analgesic [4], anti-tubercular [5], anti-glaucoma [6], anti-HIV [7], cytotoxic [8], anti-microbial [9] and anti-malarial [10] agents. The synthesis of metal sulfanilidie compounds had received much attention due to the fact that sulfanilamides were the first effective chemotherapeutic agents to be employed for the prevention and cure of bacterial infections in humans. The pharmacological activity of these types of molecules is often enhanced by complexation with metal ions [11,12]. The anti-bacterial activity of sulfonamides is confined only to microorganisms which synthesize their own folic acid [13]. The effectiveness of burn treatment seemed to depend not only in the presence of metal ion but also crucially on the nature of the material to which the metal ion is

bound [14]. Certain theories had been advanced advocating that a major portion of drug action occurred through complexation [15].

The importance of metal ions in biological systems is well known. One of the very interesting features of metal coordinated systems is the concerted spatial arrangement of the ligands around the metal ions. Among metal ions of biological importance, the Cu(II) ion presents a high number of complexes with distortion [16]. Metal complexes of sulfonamide ligands incorporating additional donor atoms from iminomethyl and phenol groups [17], iminomethyl and thiophenol groups [18] or pyridine groups [19,20] had been investigated recently.

In continuation to our work on sulfa drugs [21–23], this article involves the synthesis and characterization of Co(II), Ni(II), Cu(II) and Zn(II) complexes with four new azo sulfa drugs had been described. The solid products were characterized by elemental and thermal analyses, IR, molar conductance, magnetic moment and solid reflectance spectra measurements. The thermal decomposition of the complexes is also used to infer the structure and the different thermodynamic activation parameters are calculated.

* Corresponding author.

E-mail address: ggenidy@yahoo.com (G.G. Mohamed).

2. Experimental

All chemicals used in the preparation of the complexes and in solution studies were of the highest purity available. They included 4-aminobenzenesulfonamide (**1a**), 4-amino-*N*-1,3-thiazol-2-ylbenzenesulfonamide (**1b**), 4-amino-*N*-pyrimidin-2-ylbenzenesulfonamide (**1c**) and 4-amino-*N*-[amino(imino)methyl]benzenesulfonamide (**1d**) supplied from Sigma. Cobalt acetate tetrahydrate (BDH), copper and zinc acetate dihydrate (ProLab), and nickel chloride hexahydrate (BDH). Ethylenediaminetetracetic acid (EDTA) disodium salt, zinc oxide (Analar), and ammonium chloride and hydroxide (Merck) were used as received. The organic solvents used included absolute ethyl alcohol (BDH) and diethyl ether and dioxane (Aldrich).

Elemental analyses (C, H, N, S and M) were performed in the Microanalytical Center at Cairo University. The analyses were repeated twice. ^1H NMR spectra were carried out in $\text{DMSO-}d_6$ at 300 MHz on Varian Mercury VX spectrometer using TMS as an internal standard. The IR spectra were recorded using 1430 Perkin-Elmer FT-IR spectrometer and in wave number region $4000\text{--}400\text{ cm}^{-1}$. The spectra were recorded as KBr disks. The molar magnetic susceptibilities of the powdered samples were measured using the Faraday method (magnetic susceptibility balance–Sherwood were made by Pascal's constant using $\text{Hg}[\text{Co}(\text{SCN})_4]$ calibrant. The diffuse reflectance spectra were recorded using Shimadzu 3101pc spectrophotometer. The spectra were recorded as BaSO_4 disks. The molar conductance measurements of the complexes were carried out in DMF using a Genway 4200 conductivity meter. pH measurements were carried out using GENWAY 3020 pH meter. Thermal analyses (TGA and DTA) of the complexes were carried out in dynamic nitrogen atmosphere (20 mL min^{-1}) with a heating rate of $10\text{ }^\circ\text{C min}^{-1}$ using Shimadzu TGA-50 H and DTA-50 Hz. The percent weight loss was measured from the ambient temperature up to $1000\text{ }^\circ\text{C}$. Highly sintered $\alpha\text{-Al}_2\text{O}_3$ was used as a reference. Metal contents of the complexes were determined by titration against standard EDTA after complete decomposition of the complexes with aqua regia in a 50 mL digestion flasks.

2.1. Preparation of the azo ligands (L1 and HL2–4)

A solution of the appropriate 4-aminobenzenesulfonamide (**1a**), 4-amino-*N*-1,3-thiazol-2-ylbenzenesulfonamide (**1b**), 4-amino-*N*-pyrimidin-2-ylbenzenesulfonamide (**1c**) and 4-amino-*N*-[amino(imino)methyl]benzenesulfonamide (**1d**) (0.01 mol) in 30 mL hydrochloric acid (30%, v/v) was treated with a cold saturated solution of sodium nitrite (0.013 mol), with stirring in ice-bath for 15 min, after that the cold solutions were added to a cold solution of 2,5-diphenyl-2,4-dihydro-3H-pyrazol-3-one (**3**) (0.01 mol) in ethanol (30 mL) containing 2.0 g of sodium acetate. The reaction mixtures were stirred in ice-bath for 1 h. The solid products that formed were filtered off, washed with cold water, dried and crystallized from the proper solvent to give 4-[2-(5-oxo-1,3-diphenyl-1,5-dihydro-4H-pyrazol-4-ylidene)-hydrazino]benzenesulfonamide (L1), 4-[2-(5-oxo-1,3-diphenyl-1,5-dihydro-4H-pyrazol-4-ylidene)-

hydrazino]-*N*-1,3-thiazol-2-yl-benzenesulfonamide (HL2), 4-[2-(5-oxo-1,3-diphenyl-1,5-dihydro-4H-pyrazol-4-ylidene)-hydrazino]-*N*-pyrimidin-2-ylbenzenesulfonamide (HL3) and *N*-[amino(imino)methyl]-4-[2-(5-oxo-1,3-diphenyl-1,5-dihydro-4H-pyrazol-4-ylidene)-hydrazino]benzenesulfonamide (HL4), respectively.

2.2. Preparation of solid complexes

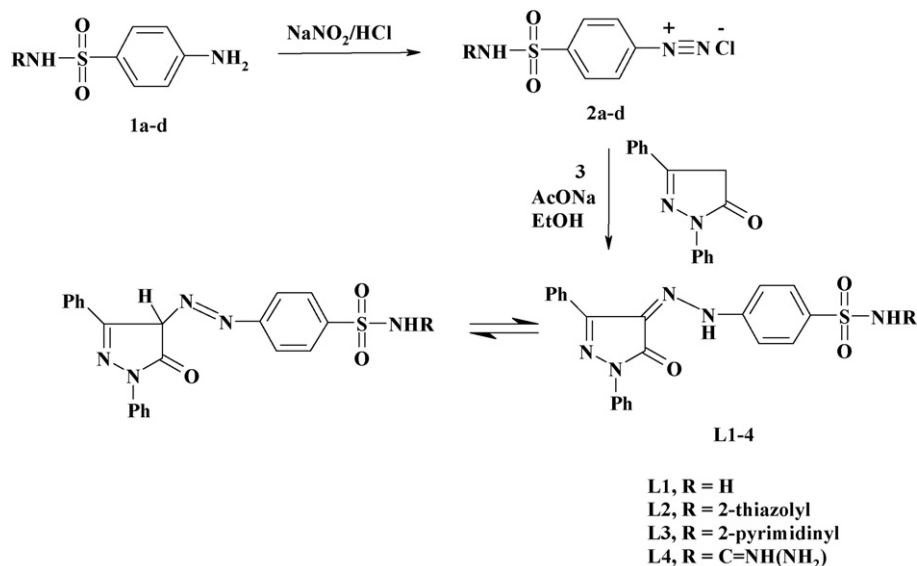
Metal complexes were synthesized by the addition of a hot ethanolic solution ($60\text{ }^\circ\text{C}$) of the appropriate metal chloride or acetate (25 mL, 0.1 mmol) to a hot ammoniacal ethanolic solution (25 mL) of azo ligands (25 mL, 0.05 mmol). The resulting mixture was stirred under reflux for 2 h and left to cool whereby the complexes were precipitated. The solid complexes were filtered, washed firstly by ethanol and then by diethyl ether and dried in vacuum desiccator over anhydrous calcium chloride.

3. Results and discussion

3.1. Preparation and characterization of the ligands

It has been found that the reaction of 4-aminobenzenesulfonamide (**1a**) with nitrous acid (NaNO_2/HCl) afforded the diazonium salt 2a, which underwent coupling reaction with 2,5-diphenyl-2,4-dihydro-3H-pyrazol-3-one (**3**) to yield the azo coupling product L1. The structure of L1 was elucidated based on elemental (Tables 1S and 2S in supplementary data) and spectral data. The ^1H NMR spectrum of L1 (Table 3S in supplementary data) indicated the signals of 4H-pyrazole and NH at $\delta = 3.49$ and 13.62 ppm, respectively, indicated that the structure of L1 is present in a mixture of the two tautomeric forms the azo and the hydrazo form. Its IR spectra (Tables 4S and 5S in supplementary data) showed the absorption bands of NH_2 , $\text{C}=\text{O}$ and $\text{N}=\text{N}$ at 3356 , 3264 , 1656 and 1547 cm^{-1} , respectively. In the same way, **1b–d** underwent diazotization and coupling with **3** to give HL2–4, as shown in Scheme 1. Compounds L1 and HL2–4 are separated in high yield (80–85%).

The aim of this study is to investigate the chelating properties of different new azo ligands towards some biologically important metals like Co(II), Ni(II), Cu(II) and Zn(II) and assign the possible structures of these complexes. The results of the elemental analyses (C, H, N, S and metal content) with the proposed molecular formulae are presented in Tables 1S and 2S in supplementary data. The results obtained are in good agreement with those calculated for the suggested formulae. 2:1 (M: L2 or L3 or L4) solid chelates are isolated and found to have the general formulae $[(\text{MX}_2)_2(\text{HL2 or HL3})(\text{H}_2\text{O})_m]\cdot n\text{H}_2\text{O}$ and $[\text{M}_2\text{X}_3(\text{L4})(\text{H}_2\text{O})]\cdot n\text{H}_2\text{O}$; M = Co(II), Ni(II) and Cu(II) (X = Cl) and Zn(II) (X = AcO); $m = 4$ and $n = 0\text{--}3$. While L1 form 1:1 (M:L1) complexes with the formula $[\text{MX}_2(\text{L1})(\text{H}_2\text{O})_m]\cdot n\text{H}_2\text{O}$; M = Co(II), Ni(II) and Cu(II) (X = Cl) and Zn(II) (X = AcO); $m = 0\text{--}2$ and $n = 0\text{--}2$. The solid complexes are prepared and characterized by different tools of analyses like IR, molar conductance, magnetic moment, solid reflectance and thermal analyses (TGA and DTA) to through more light on the coor-



Scheme 1.

dination behaviour of these ligands towards some biologically active metals under study.

3.2. Infrared spectra and mode of bonding

The IR spectra of the free ligands and their metal complexes were carried out in the range of 4000–400 cm^{-1} and listed in Tables 4S and 5S in supplementary data. The stretching vibration band; $\nu(\text{NH})$, of the sulfonamide group, which found at 3440–3448 cm^{-1} in the free ligands, was disappeared or hidden under the peak of water molecules. The presence of coordinated water molecules renders it difficult to confirm the enolization of the sulfonamide group. The SO_2 group modes of the HL2–4 ligands appear as sharp bands at 1335–1337 and 1140–1160 cm^{-1} ($\nu_{\text{asym}}(\text{SO}_2)$) and ($\nu_{\text{sym}}(\text{SO}_2)$), respectively. In the complexes, the asymmetric and symmetric modes are shifted to 1312–1326 and 1122–1167 cm^{-1} , respectively, upon coordination to the transition metals [21,22]. The blue shift of the SO_2 stretching vibration to lower frequencies may be attributed to the transformation of the sulfonamide ($-\text{SO}_2\text{NH}$) to give the enol form ($-\text{SO}(\text{OH})=\text{N}$) as a result of complex formation to give more stable six-membered ring [21,22]. The two bands at 1340 and 1154 cm^{-1} for asymmetric and symmetric SO_2 stretching vibrations groups for L1 ligand are slightly shifted to higher or lower frequencies upon chelates. As the SO_2 group is not involved in metal bonding, this shift to higher or lower frequencies must be related to important hydrogen bonding effects. Another possible explanation for this shift may be the electronic density changes on the sulfur atom and in the ring after complex formation.

The strong bands at 1545–1552 cm^{-1} in the spectra of the free ligands may be attributed to the azo group stretching vibration. These bands are shifted to higher or lower frequencies as the results of complex formation. This indicates the involvement of the azo group in chelate formation. The strong and sharp bands at 1659 and 1660 cm^{-1} of the thiazolyl and pyrimidine-N; $\nu(\text{C}=\text{N})$,

in the free HL2 and HL3 ligands, respectively, are shifted to 1642–1670 and 1652–1672 cm^{-1} in the metal complexes. This indicates the participation of the thiazolyl and pyrimidine-N in complex formation. A sharp bands due to the $\nu(\text{C}=\text{O})$ stretching vibration of pyrazolone ring appeared at 1656–1743 cm^{-1} in the free ligands. These bands are shifted to 1640–1753 cm^{-1} in the spectra of the metal complexes. These shifts refer to the coordination through pyrazolone O atom.

The appearance of bands in the complexes in the 588–665 and 535–577, and 440–485 and 426–448 cm^{-1} regions which may be assigned to the $\nu(\text{M}-\text{O})$ and $\nu(\text{M}-\text{N})$ stretching vibrations of the coordinated O and N atoms of the ligands, respectively.

Therefore, from the IR spectra, it is concluded that L1 behaves as neutral bidentate ligand while HL2–3 ligands behave as neutral tetradentate and HL4 ligand behaves as a uni-negatively tetradentate ligand. They coordinated to the metal ions via the azo N, carbonyl O, enolic sulfonamide OH and pyrazole or thiazole-N.

3.3. Molar conductance data

The molar conductance of the solid complexes (Λ_m , $\Omega^{-1} \text{cm}^2 \text{mol}^{-1}$) was calculated. The DMF solubility of the above complexes made calculations of the molar conductivity (Λ_m) of 10^{-3}M solution at 25 °C possible. The data in Tables 1S and 2S in supplementary data show that the molar conductance are of relatively low values for Co(II), Ni(II), Cu(II) and Zn(II), indicating the non-electrolytic nature of these complexes. Therefore, the molar conductance data confirm the results of the elemental analyses and IR spectral data.

3.4. Solid reflectance spectra and magnetic susceptibility measurements

For Co(II) complexes with L1, HL2 and HL3 ligands, the reflectance spectra show three bands at 12,820–13,513,

17,421–18,484 and 22,471–23,255 cm^{-1} which are assigned to ${}^4\text{T}_{1g}(\text{F}) \rightarrow {}^4\text{T}_{2g}(\text{F})$, ${}^4\text{T}_{1g}(\text{F}) \rightarrow {}^4\text{E}_{2g}(\text{F})$ and ${}^4\text{T}_{1g}(\text{F}) \rightarrow {}^4\text{T}_{2g}(\text{P})$ transitions, respectively, which assume an octahedral geometry for Co(II) complex [24–26]. The band at 25,641–26,595 cm^{-1} , refers to LMCT [25]. Co(II) complexes have μ_{eff} of 4.69–4.92 which assumes a high spin octahedral geometry [25], may arise from spin–spin coupling and/or crystal distortion.

Three spin allowed transition bands, ${}^4\text{A}_2(\text{F}) \rightarrow {}^4\text{T}_2(\text{F})$ (ν_1); ${}^4\text{A}_2(\text{F}) \rightarrow {}^4\text{T}_1(\text{F})$ (ν_2) and ${}^4\text{A}_2(\text{F}) \rightarrow {}^4\text{T}_1(\text{P})$ (ν_3) are expected for tetrahedral symmetry of Co(II) complex with HL4 ligand. In the present case, only two bands at 13,071 and 17,452 cm^{-1} have been observed in the diffuse reflectance spectrum of Co(II) complex which is assigned to ν_2 and ν_3 , respectively, as ν_1 occurs in the range 3000–5000 cm^{-1} [25]. The band at 25,974 cm^{-1} , refers to LMCT [22,25]. The Co(II) complex has magnetic moment of 5.66 B.M. which is in agreement with the values for high tetrahedral Co(II) complexes [26].

The electronic spectra of the Ni(II) complexes of L1, HL2 and HL3 ligands displays three bands in the solid reflectance spectra as follows: 12,850–13,368 cm^{-1} ; ${}^3\text{A}_{2g} \rightarrow {}^3\text{T}_{2g}$ (ν_1), 15,698–16,420 cm^{-1} ; ${}^3\text{A}_{2g} \rightarrow {}^3\text{T}_{1g}(\text{F})$ (ν_2) and 17,361–17,543 cm^{-1} ${}^3\text{A}_{2g} \rightarrow {}^3\text{T}_{1g}(\text{P})$ (ν_3). The band at 25,252–26,809 cm^{-1} , refers to LMCT [25]. This indicates octahedral geometry of the Ni(II) complex [25,27]. The Ni(II) complexes have μ_{eff} of 3.53–4.26 B.M., which suggest an octahedral geometry [25].

The Ni(II) complex of HL4 ligand exhibits medium intensity broad bands at 13,888 and 20,092 cm^{-1} , attributed to the ${}^1\text{A}_{1g} \rightarrow {}^1\text{A}_{2g}$ and ${}^1\text{A}_{1g} \rightarrow {}^1\text{B}_{1g}$ transitions, respectively [27]. The observed band in the region 15,698 cm^{-1} ; attributed to the ${}^3\text{T}_1(\text{F}) \rightarrow {}^3\text{T}_1(\text{P})$ transition, reveals that Ni(II) has tetrahedral configuration [27]. The complex has μ_{eff} of 4.76 B.M., which is consistent with the tetrahedral geometry with an orbital contribution to magnetic moment [26].

The reflectance spectra of the Cu(II) complexes of L1, HL2 and HL3 ligands consists of a broad and low intensity shoulder band at 15,873–17,452 cm^{-1} that forms part of the charge transfer band. The ${}^2\text{E}_g$ and ${}^2\text{T}_{2g}$ states of the octahedral Cu(II) ion (d^9) split under the influence of the tetragonal distortion to three transitions; ${}^2\text{B}_{1g} \rightarrow {}^2\text{B}_{2g}$; ${}^2\text{B}_{1g} \rightarrow {}^2\text{E}_g$ and ${}^2\text{B}_{1g} \rightarrow {}^2\text{A}_{1g}$ to remain unresolved in the spectra [28]. It is concluded that, all three transitions lie within the single broad envelope centered at the same range previously mentioned. This assignment is in agreement with the general observation that Cu(II) d–d transitions are normally close in energy [25]. The Cu(II) complex has $\mu_{\text{eff}} = 1.83$ –196 B.M., assuming a distorted octahedral structure [28].

The solid reflectance spectrum of the Cu(II) complex with HL4 ligand shows a broad band at 15,673 cm^{-1} assigned to ${}^2\text{E}_g \rightarrow {}^2\text{T}_{2g}$ transition and broad band at 13,513 cm^{-1} which is assigned to ${}^2\text{B}_{1g} \rightarrow {}^2\text{A}_{1g}$ transition as well as a shoulder band at 17,482 cm^{-1} characteristic of a square planer geometry for Cu-complex [28]. In addition, a moderately intense peak observed at 26,315 cm^{-1} is due to ligand to metal charge transfer transition [28]. The μ_{eff} value of the Cu(II) complex is 2.05 B.M., which assume a tetrahedral geometry for this complex [26].

The Zn(II) complexes are diamagnetic and are likely to be octahedral with HL2 ligand and tetrahedral with L1, HL3 and HL4 ligands.

3.5. Thermal analysis data

The TGA and DTA data of the thermal decomposition of the complexes are listed in Tables 6S and 7S in supplementary data. The thermodynamic parameters for the different decomposition steps are deduced using Coats–Redfern method and listed in Tables 8S and 9S in supplementary data, where the average values of these parameters are those considered in the discussion. The correlations between the different decomposition steps of the complexes with the corresponding weight losses are discussed in terms of the proposed formulae of the complexes as follows:

The Co(II), Ni(II), Cu(II) and Zn(II) complexes of L1 ligand were thermally decomposed in the same manner. They decomposed in three to four successive decomposition steps within the temperature range 30–800 °C. The Co(II) and Ni(II) complexes lose their water of hydration within the temperature range 30–110 °C with an estimated mass loss of 5.66% (calcd. 5.93%) and 6.15% (calcd. 5.93%) for Co(II) and Ni(II) complexes, respectively. The activation energy of this dehydration step is 63.35 and 34.96 kJ mol^{-1} . The complexes lose coordinated water, HCl, $1/2\text{O}_2$, CH_4 and 2CO_2 gases within the temperature range 100–320 °C with an estimated mass loss of 17.55% (calcd. 17.63%), 17.13% (calcd. 17.63%), 16.93% (calcd. 16.74%) and 20.35% (calcd. 20.07%) for Co(II), Ni(II), Cu(II) and Zn(II) complexes, respectively. The energies of activation were 102.6, 88.64, 62.52 and 42.85 kJ mol^{-1} for the Co(II), Ni(II), Cu(II) and Zn(II) complexes, respectively. The last steps found within the temperature range 280–800 °C with an estimated mass loss 64.75% (calcd. 64.09%), 63.79% (calcd. 64.09%), 61.12% (calcd. 60.88%) and 66.58% (calcd. 66.16%) for Co(II), Ni(II), Cu(II) and Zn(II) complexes, respectively, which is responsibly accounted for the pyrolysis of L1 molecule with a final oxide residue of CoO, NiO, CuO and ZnO. The activation energy is 182.5, 159.8, 107.7 and 135.9 kJ mol^{-1} . The DTA data listed in Tables 7S and 8S in supplementary data show the exo and endothermic peaks accompanying the processes of dehydration, anions and coordinated water removal and decomposition of the ligand molecules.

The metal complexes of HL2 ligand were thermally decomposed in five successive decomposition steps. The first estimated mass loss of 3.51–6.68% within the temperature range 30–140 °C may be attributed to the liberation of hydrated water molecules (calcd. 3.69–6.08%). The activation energy of this step is 43.45–73.05 kJ mol^{-1} . The second and third steps occurred within the temperature range 100–400 °C with an estimated mass loss 14.00–24.60% (calcd. 13.43–24.10%) which is accounted for the removal of coordinated water, HCl, O_2 , CH_4 and CO_2 gases, with an activation energy of 65.89–92.49 kJ mol^{-1} . The last two steps occur within the temperature range 320–750 °C with an estimated mass loss 52.31–66.77% (calcd. 52.93–66.29%) and activation energies of 137.4, 177.2, 117.6 and 172.4 kJ mol^{-1} for Co(II), Ni(II),

Cu(II) and Zn(II) complexes, respectively, which correspond to the loss of ligand molecule leaving metal oxide residue.

The TGA data of the metal complexes of HL3 ligand (Tables 6S and 7S in supplementary data) indicated that the complexes are thermally decomposed in three to four steps. The first decomposition step represent the loss of coordinated water, HCl and O₂ gases in the Co(II) and Ni(II) complexes only. While the first decomposition step in Cu(II) and Zn(II) complexes correspond to the loss of coordinated water molecules within the temperature range 40.0–250 °C. The energy of activation of this step is 43.65, 23.95, 46.87 and 64.10 kJ mol⁻¹ for Co(II), Ni(II), Cu(II) and Zn(II) complexes, respectively. The remaining steps found in the temperature range 280–750 with an estimated weight loss of 56.95% (calcd. 56.09%) and 56.35% (calcd. 56.09%) and activation energy of 122.4 and 72.47 kJ mol⁻¹ for Co(II) and Ni(II) complexes, respectively, is due to the decomposition of HL3 molecule leaving metal oxide residues (CoO and NiO). The last steps occur within the temperature range 100–900 °C with an estimated mass loss 73.21% (calcd. 72.91%) and 78.28 (calcd. 77.98%) for Cu(II) and Zn(II) complexes, respectively, which are reasonably accounted for the liberation HCl, CH₄, CO₂ and ligand molecule leaving Cu₂O and ZnO residues. The energy of activation of this step is 89.67 and 118.3 kJ mol⁻¹ for Cu(II) and Zn(II) complexes, respectively.

The metal complexes of HL4 ligand are thermally decomposed in three to four successive decomposition steps. The first two steps with an estimated mass loss of 22.85–29.09% (calcd. 23.60–28.13%) within the temperature range 30–290 °C can be attributed to the liberation of hydrated water, HCl, O₂, H₂, CH₄ and CO₂ gases. The energy of activation of this step is 50.22, 42.33, 65.25 and 41.98 kJ mol⁻¹ for Co(II), Ni(II), Cu(II) and Zn(II) complexes, respectively. The remaining steps found within the temperature range 250–900 °C with an estimated weight loss of 56.93% (calcd. 56.58%), 56.85% (calcd. 56.58%), 57.83% (calcd. 57.26%) and 51.69% (calcd. 52.13%) and activation energy of 117.6, 95.98, 155.3 and 115.6 kJ mol⁻¹ for Co(II), Ni(II), Cu(II) and Zn(II) complexes, respectively, is attributed to the removal of ligand molecule leaving MO as metallic residue.

3.6. Kinetic analysis

The thermodynamic activation parameters of decomposition processes of dehydrated complexes namely activation energy (E^*), enthalpy (ΔH^*), entropy (ΔS^*) and Gibbs free energy change of the decomposition (ΔG^*) were evaluated graphically by employing the Coats–Redfern relation [29]:

$$\log \left[\frac{\log \{W_f / (W_f - W)\}}{T^2} \right] = \log \left[\frac{AR}{\theta E^*} \left(1 - \frac{2RT}{E^*} \right) \right] - \frac{E^*}{2.303RT} \quad (1)$$

where W_f is the mass loss at the completion of the reaction, W the mass loss up to temperature T , R the gas constant, E^* the activation energy in kJ mol⁻¹, θ the heating rate and $(1 - (2RT/E^*)) \cong 1$. A plot of the left-hand side of Eq. (1) against

$1/T$ gives a slope from which E^* was calculated and A (Arrhenius factor) was determined from the intercept. The entropy of activation (ΔS^*), enthalpy of activation (ΔH^*) and the free energy change of activation (ΔG^*) were calculated. The calculated values of E^* , A , ΔS^* , ΔH^* and ΔG^* for the decomposition steps are given in Tables 8S and 9S in supplementary data. According to the kinetic data obtained from the DTG curves, all the complexes have a negative entropy, which indicates that the complexes are formed spontaneously.

3.7. Structural interpretation

The structural information from these complexes is in agreement with the data reported in this paper based on the elemental and thermal analyses, IR and solid reflectance spectra, molar conductance, and magnetic moment measurements. Consequently, the structures proposed are based on octahedral, tetrahedral and square planar geometric structures. The azo ligands coordinate via the azo N, carbonyl O, enolic sulfonamide OH and pyrazole or thiodiaza N groups forming two binding chelating sites. According to the above data, the structures of the complexes are shown in Figs. 1S–3S in supplementary data.

Supplemental information

Tables 1S and 2S contains the analytical and physical data of the complexes. Table 3S contains the ¹H NMR spectra of the ligands while Tables 4S and 5S contain the IR data. Tables 6S and 7S contain the TGA results while Tables 8S and 9S have the kinetic data. Figs. 1S–3S contain the structures of the isolated solid complexes.

Appendix A. Supplementary data

Supplementary data associated with this article can be found, in the online version, at doi:10.1016/j.saa.2007.01.034.

References

- [1] Y. Funahashi, N.H. Sugi, T. Semba, Y. Yamamoto, S. Hamaoka, N. Tsukahara-Tamai, Y. Ozawa, A. Tsuruoka, K. nara, K. Takahashi, T. okabe, J. Kamata, T. Owa, N. ueda, T. Haneda, M. Yonaga, K. Yoshimatsu, T. Wakabayashi, Cancer Res. 62 (2002) 6116.
- [2] T. Semba, Y. Funahashi, N. Ono, Y. Yamamoto, N.H. Sugi, M. Asada, K. Yoshimatsu, T. Wakabayashi, Clin. Cancer Res. 10 (2004) 1430.
- [3] J. Sławiński, M. Gdaniec, Eur. J. Med. Chem. 40 (2005) 377.
- [4] Q. Chen, P.N.P. Rao, E.E. Knaus, Bioorg. Med. Chem. 13 (2005) 2459.
- [5] A.K. Gadad, M.N. Noolyi, R.V. Karpoornath, Bioorg. Med. Chem. 12 (2004) 5651.
- [6] V.K. Agrawal, S. Bano, C.T. Supuran, P.V. Khadikar, Eur. J. Med. Chem. 39 (2004) 593.
- [7] C.M. Yeung, L.L. Klein, C.A. Flentge, J.T. Randolph, C. Zhao, M. Sun, T. Dekhtyar, V.S. Stoll, D.j. Kempf, Bioorg. Med. Chem. Lett. 15 (2005) 2275.
- [8] I. Encío, Dj. Morr , R. Villar, Mj. Gil, V. Mart nez-Merino, Br. J. Cancer 92 (2005) 690.
- [9] M.J. Nieta, F.L. Alovero, R.H. Manzo, M.R. Mazzieri, Eur. J. Med. Chem. 40 (2005) 361.
- [10] J.N. Dom nguez, C. Le n, J. Rodr guez, N.G. de Dom nguez, J. Gut, P.J. Rosenthal, Il Farmaco 60 (2005) 307.

- [11] A. Bult, H. Sigel, *Metal Ions in Biological Systems*, vol. 116, Marcel Dekker, New York, 1983, p. 261.
- [12] J. Casanova, G. Alzuet, S. Ferrer, J. Borrás, S.G. Granda, E.J. Carreno, *J. Inorg. Biochem.* 51 (1983) 689, and references therein.
- [13] O.P. Agrawal, *Synthetic Organic Chemistry*, Goel Publishing House, Merrut, 1985.
- [14] A.G. Raso, J.J. Fiol, S. Rego, A.I. Lopez, E. Molins, E. Espinosa, E. Borrás, G. Alzuet, J. Borrás, A. Castineiras, *Polyhedron* 19 (2000) 991.
- [15] R.C. Maurya, P. Patel, *Spectrosc. Lett.* 32 (2) (1999) 233.
- [16] L. Gutierrez, G. Alzuet, J. Borrás, M.L. Gonzalez, F. Sanz, A. Castineiras, *Polyhedron* 20 (2001) 703.
- [17] A.D. Garnovskii, A.S. Burlok, D.A. Garnovskii, I.S. Vasilchenko, A.S. Antsyshkina, G.D. Sadekov, A. Sousa, J.A.G. Vazquez, J. Romero, M.L. Duran, A.S. Pedrares, C. Gomez, *Polyhedron* 18 (1999) 863.
- [18] A.S. Burlok, A.S. Antsyshkina, J. Romero, D.A. Garnovskii, J.A.G. Vazquez, A.D. Garnovskii, *Russ. J. Inorg. Chem.* 40 (1995) 1427.
- [19] S. Cabaleiro, J. Castro, J.A.G. Vazquez, J. Romero, A. Sousa, *Polyhedron* 19 (2000) 1607.
- [20] J. Castro, S. Cabaleiro, P.P. Lourido, J. Romero, J.A.G. Vazquez, A. Sousa, *Polyhedron* 20 (2001) 2329.
- [21] G.G. Mohamed, C.M. Sharaby, *Spectrochim. Acta, Part A* 66 (2007) 949.
- [22] C.M. Sharaby, G.G. Mohamed, M.M. Omar, *Spectrochim. Acta, Part A* 66 (2007) 935.
- [23] M.A.M. Gad-Elkareem, *Afinidad* 63 (2006) 247.
- [24] M.M. Moustafa, *J. Therm. Anal.* 50 (1997) 463.
- [25] A. Kapahi, K.P. Pandeya, R.P. Singh, *J. Inorg. Nucl. Chem.* 40 (1987) 355.
- [26] F.A. Cotton, G. Wilkinson, C.A. Murillo, M. Bochmann, *Advanced Inorganic Chemistry*, 6th ed., Wiley, New York, 1999.
- [27] B.M. Badiger, S.D. Angadi, S.A. Patil, V.H. Kulkarni, *Ind. J. Chem. Soc.* 72 (1995) 80.
- [28] (a) M.F. Eskander, T.E. Khalil, R. Werner, W. Haase, I. Svoboda, H. Fuess, *Polyhedron* 19 (2000) 949;
(b) P.S. Reddy, K.H. Reddy, *Polyhedron* 19 (2000) 1687.
- [29] A.W. Coats, J.P. Redfern, *Nature* 20 (1964) 68.